Proceedings of the 2002 IEEE
International Conference on Robotics & Automation
Washington, DC • May 2002

# Trajectory Stabilization for a Planar Carangiform Robot Fish

Kristi A. Morgansen†, Patricio A. Vela†, Joel W. Burdick‡ [1]

†Control and Dynamical Systems ‡Mechanical Engineering
California Institute of Technology, Mail Code 107-81, Pasadena, CA, 91125
{kristi,pvela}@cds.caltech.edu, jwb@robotics.caltech.edu

**Abstract:** *This paper considers the task of trajectory stabilization for a fish-like robot by means of feedback. We use oscillatory control inputs and apply correction signals at the endpoints of each periodic input signal. Such a strategy can be proven to cause the system to converge to a desired trajectory. We present a specific model of a planar carangiform fish, and verify the stabilization results with simulations and with experiment on a planar robotic fish system that is propelled using carangiform-like movements.*

## 1 Introduction

This paper investigates fish-like robots that propel themselves by changes in their shape, rather than by the use of propellers and maneuvering surfaces. We particularly focus on the task of stabilizing these robots to follow a given trajectory. Our stabilization approach is based on the authors' recently developed averaging methods for control of nonholonomic mechanical systems [21]. This paper reviews these techniques, applies them to a particular model of planar carangiform-like robot fish, and experimentally verifies the method on a planar three-link carangibot.

Underwater locomotion has long been studied by the biological community (see e.g., [7, 17, 11]). In the past several years, robotic engineers have been inspired by this research to construct mechanisms that mimic the behavior of swimming lifeforms. The motivation for this work comes from the potentially superior stealth, maneuverability, and efficiency of fish-like vehicles as compared to conventional propeller-driven underwater vehicles.

While a variety of propulsion schemes have been investigated (e.g., amoeba-like propulsion [13, 6]), most investigations of fish-like swimming have focused on *carangiform*-like swimming. In carangiform swimming, the front two-thirds of the fish's body moves in a largely rigid way, while the propulsive body movements are confined mainly to the rear third of the body—primarily the tail. Some of the most impressive natural swimmers propel themselves by the carangiform mode of swimming, and the carangiform movement is one of the easiest to replicate mechanically. This paper focuses on carangiform-like robot swimmers. While we stabilize a planar version of carangiform swimming rather than a full three dimensional system, in fact the mechanics of carangiform swimming are largely dominated by the fluid mechanics in the horizontal plane. Furthermore, the control theoretic techniques that we use for stabilization are quite general, and can be applied not only to other swimming models but to any underactuated system. Hence, our results have relatively wide application and possibilities for extension.

Previous work on carangiform-like swimming has focused on the mechanical design of such swimmers [2, 20], on the fluid flow patterns involved in carangiform swimming [22, 10], or on issues of drag reduction [3]. The work reported in this paper differs from most prior work in that it focuses on rigorous feedback stabilization of fish-like robots. Our purpose is not to focus on efficiency or maneuverability, however our approach does not preclude the such considerations. As discussed in [15], the equations of motion for this system have an uncontrollable linearization which prevents the use of linear system stability tools. Additionally, the combination of the complicated dynamics structure and the use of time-varying inputs makes the application of methods such as Lyapunov stability criteria intractable. There have been almost no prior efforts to develop feedback stabilizing controllers for such vehicles although Saimek and Li [18] have studied and implemented an optimal control approach on a fish-like vehicle. Our approach applies to more general and complicated fluid models, and we can prove the stability of our method. The tools we use are quite mathematical, but are necessary for a complete study of stability for the class of linearly uncontrollable underactuated mechanical systems into which the carangiform robot falls. This paper builds upon prior work by the authors and their collaborators on the subjects of body/fluid modeling for control design [8, 14], open loop trajectory generation [15], and the development of an experimental carangiform test-bed that operates in biologically appropriate hydrodynamic regimes [14].

The paper is organized as follows. The next section dis-

[1]This work was supported in part by the National Science Foundation through an Engineering Research Center grant (NSF9402726) and through NSF grant CMS-9502224.

cusses the model we use for our mechanism, as well as the characteristics of the general class of underactuated mechanical systems into which this vehicle falls. Our results apply to all such mechanisms. Sec. 3 summarizes theoretical averaging and tracking results derived in [21], which we then apply in simulation and experiment to our carangiform-like robot in Sec. 4.

## 2 System Model

The simple fish robot studied in this paper and the related earlier works [8, 12, 14, 15] consists of a planar three link mechanism immersed in water (see Sec. 4 for details). A simple diagram of the system is shown in Fig. 1. The position and orientation of the body's center of mass relative to a body-fixed reference frame are denoted equivalently by $\chi = [x, y, \theta]$ or $g \in SE(2)$ with the body-fixed velocity given by $\xi = [\dot{\xi}_x, \dot{\xi}_y, \dot{\xi}_\theta]$ where $\dot{g} = g\xi$. We do not assume that the body's center of mass coincides with its geometric center. The orientation of the peduncle and tail joints are denoted by $r = [\psi_1, \psi_2]$, and are measured with respect to the main body reference frame. The equations of motion for an actuated system in a ideal incompressible fluid are given by Hamel's equations

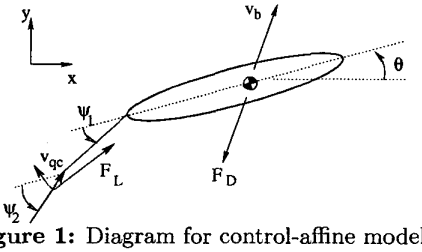

**Figure 1:** Diagram for control-affine model.

$$\begin{aligned} \frac{d}{dt}\frac{\partial \mathcal{L}}{\partial \xi} &= ad^*_\xi \frac{\partial \mathcal{L}}{\partial \xi} + F_\xi = \frac{\partial \mathcal{L}}{\partial t} \times \xi + F_\xi \\ \frac{d}{dt}\frac{\partial \mathcal{L}}{\partial \dot{r}} &= \frac{\partial \mathcal{L}}{\partial r} + F_r \end{aligned} \tag{1}$$

where $F_\xi = F_\xi(, r, \xi, \dot{r})$ and $F_r = F_r(r, \dot{r}, t)$ are forces acting on the mechanism and $\mathcal{L}$ is the system Lagrangian which includes both physical and added mass effects. The forces acting on the system are lift on the tail and form drag on the body. We could also include lift on the body, form drag on the tail and skin friction, but the comparative size of these terms is small. As discussed in [15], we take the drag for a translating and rotating plate to be given by

$$F_D = \frac{\rho C_d h}{2} \int_{\frac{l}{2}-a}^{\frac{l}{2}+a} \|\xi((a+s)e_1) \times e_1\| \xi((a+s)e_1) ds$$

and the associated moment to be

$$M_D = \frac{\rho C_d h}{2} \int_{\frac{l}{2}-a}^{\frac{l}{2}+a} \|\xi((a+s)e_1) \times e_1\| (\xi((a+s)e_1) \times e_1) s ds$$

where $\rho$ is the density of water, $l$ is the length of the plate, $C_d$ is the drag coefficient for the plate when its velocity aligns with the $y$ direction, $h$ is the height of the plate, $a$ is the difference in position between the center of mass and center of geometry of the plate, and $\xi((a+s)e_1)$ is the body-fixed velocity of the plate at the point $a+s$ along the body. The value of $s$ varies from $\frac{l}{2} - a$ to $\frac{l}{2} + a$, and the unit vector $e_1$ point in the direction of the body-fixed $x$ axis. The lift acting on a flat plate is given by

$$F_L = \pi \rho A (\xi_{qc} \times e_t) \times \xi_{qc}$$

where $\xi_{qc}$ is the velocity at the quarter chord point on the plate measured in the main body coordinate frame, $e_t$ is a unit vector pointing along the plate toward its leading edge, and $A$ is the area of the plate.

Collecting these terms results in equations of the form

$$M(q) \begin{bmatrix} \dot{\xi} \\ \ddot{r} \end{bmatrix} - C(q, \xi, \dot{r}) = \begin{bmatrix} F_{L,t,x} + F_{D,b,x} \\ F_{L,t,y} + F_{D,b,y} \\ [x_t, y_t] \times [F_{L,t,x}, F_{L,t,y}] + M_{D,b} \\ u_1 \\ u_2 \end{bmatrix}$$

where $q = [\chi, r] \in \mathbb{R}^5$, $M(q)$ is the mass matrix, $C(q, \xi, \dot{r})$ are Coriolis forces, $x_t$, $y_t$ is the position of the tail quarter chord point with respect to the body, and $u_i(t)$ are control functions. We have decomposed the lift and drag into the basis elements denoted by the subscripts $x$ and $y$. This system can be written in the slightly more abstract form of an actuated mechanical system without potential forces:

$$M(q)\ddot{q} + C(q, \dot{q}) = E(q, \dot{q}) + \sum_{a=1}^{m} Y_a(q) u^a(t)$$

where $E$ contains our lift and drag forces and $Y$ are control vector fields. For the purposes of the system studied in this paper, $E$ will have the form $-\tilde{E}(q, \dot{q})\dot{q}$ and we can rewrite the above equations as

$$\ddot{q} = S(q, \dot{q}) + Y_0(q, \dot{q}) - D(q)\dot{q} + Y_a(q)(1/\epsilon)v^a(t) \tag{2}$$

where $S(q, \dot{q}) = -M^{-1}(q)C(q, \dot{q})$, $D(q)\dot{q} = M^{-1}(q)\tilde{E}(q)\dot{q}$. The term $Y_a(q)$ represents the time-varying portion of $M^{-1}(q)Y(q)u(t)$, while the term $Y_0(q, \dot{q})$ represents the time-invariant terms. We can then convert the system to a first order state space representation by choosing $x = [q, \dot{q}] \in \mathbb{R}^{2n}$ and

$$Z_g(x) = \begin{bmatrix} \dot{q} \\ S(q, \dot{q}) + Y_0(q, \dot{q}) \end{bmatrix}, \; Y_a^{\text{lift}}(x) = \begin{bmatrix} 0 \\ Y_a(q) \end{bmatrix}$$
$$D^{\text{lift}}(x) = \begin{bmatrix} 0 \\ D(q)\dot{q} \end{bmatrix},$$

so that we have

$$\dot{x} = Z_g(x) - D^{\text{lift}}(x) + Y_a^{\text{lift}}(x) u^a(t).$$

The vector fields $Z_g(x)$, $D^{\text{lift}}(x)$, and $Y_a^{\text{lift}}(x)$ belong to the set of scalar functions on $\mathbb{R}^{2n}$ which are arbitrary functions of $q$ and homogeneous polynomials in

$\{\dot{q}^1, \ldots, \ldots, q^n\}$ of degree 1, 0, and $-1$ respectively. One can use these homogeneity properties to show that

$$\left[Y_a^{\text{lift}}, Y_b^{\text{lift}}\right] = 0, \quad < Y_a : Y_b >^{\text{lift}} = [Y_b^{\text{lift}}, [Z_g, Y_a^{\text{lift}}]]$$

where $< Y_a : Y_b >$ is the *symmetric product* between $Y_b$ and $Y_a$. For details concerning symmetric products see [9] and the references therein. Henceforth, this paper will make assumptions on the vector fields of Eq. (2) which are a slight generalization of these observations.

Whenever the Jacobi-Lie brackets between input vector fields of a control system vanish (as is true for mechanical systems)

$$[Y_a, Y_b] = 0 \tag{3}$$

the Jacobi identity implies that $[Y_a, [S, Y_b]] = [Y_b, [S, Y_a]]$. Hence, one naturally has a symmetric product regardless of the control system's inherent homogeneous structure

$$\langle Y_a \ : \ Y_b \rangle = [Y_b, [S, Y_a]] \tag{4}$$

Under the appropriate conditions, the above symmetric product simplifies to the one arising in mechanical systems [9, 5]. Systems with the structure

$$x(t) = S(x) + Y_0(x) + D(x) + Y_a(x)(1/\epsilon)v^a(t)$$

with $x(0) = x_0$ and Eqs. (3)-(4) in effect, which we will refer to as *simple mechanical systems*, are the focus of the results in the following section. This model holds for all mechanical systems as well as many nonmechanical systems.

## 3 Nonlinear Control Background

Generically, robotic fish are underactuated mechanical systems whose governing equations are highly nonlinear. While there is a large body of literature on motion generation and stabilization for underactuated nonholonomic systems via periodic inputs (e.g. [19, 16]), most of this prior work applies to driftless control systems or applies to the setting where only first order effects are present (e.g. [5, 4]). As discussed in [15], the type of robot in Sec. 2 does not fall into these categories due to the presence of inertial terms and second-order effects. Additionally, one could argue that many similar swimming mechanisms that locomote via changes in shape will demonstrate a need for second-order or higher methodology.

To this end, this section reviews some recently developed techniques for stabilizing systems that require higher order methods. These methods are based on the use of oscillatory feedback and are related to the ideas in [5, 4]. We quote results, whose proofs can be found in [21]. These general results are subsequently applied to a specific carangiform robot model.

### 3.1 Averaging

To examine system response under the application of oscillatory actuation. We begin by rewriting the dynamical system (2) as

$$\dot{x} = f(x) + g(x,t), \ x(0) = x_0$$

where $g(x,t)$ is a $T$-periodic function in $t$ and represents the action of control inputs. Our results use the standard form for a high amplitude, high frequency vibrational control system

$$\dot{x} = f(x) + (1/\epsilon)g(x, t/\epsilon)$$

with $\epsilon$ small. Transforming time, $t/\epsilon \mapsto \tau$, to obtain

$$\frac{\mathrm{d}x}{\mathrm{d}\tau} = \epsilon f(x) + g(x,\tau)$$

gives a system where $f(x)$ is a perturbation to the primary vector field $g(x,\tau)$ and $\tau$ is the time variable. Define the following

$$\begin{aligned} F(y,\tau) &= \epsilon \left((\Phi_{0,\tau}^g)^* f\right)(y) \\ \bar{F}(y) &= \tfrac{1}{T}\textstyle\int_0^T F(y,\tau)d\tau \end{aligned} \tag{5}$$

where $\Phi_{0,\tau}^g(x_0)$ is the solution to

$$\dot{x} = g(x,\tau), \ x(0) = x_0.$$

According to the variation of constants formula, the solution $x(t)$ is given exactly by

$$x(\tau) = \Phi_{0,\tau}^g(y(t))$$

or in differential equation form by,

$$\dot{x} = g(x,\tau), \ x(0) = y(\tau)$$

where $\{y(t), t \in [0,T]\}$ is the solution to the system $\dot{y} = F(y,\tau)$ with $y(0) = x_0$ and $F(y,\tau)$ as in Eq. (5).

We are primarily concerned with the average, or net motions, that a robot fish achieves with periodic forcing. Hence, it is convenient and suitable to compute an approximate solution that arises from the first-order averaged evolution equation:

$$\dot{z} = \epsilon \bar{F}(z).$$

and to understand the relationship between the predictions of the averaged and original systems. Higher order averaging is required when systems have zero average (whereby higher order terms dominate the dynamics) or when they require iterated brackets for control.

To compute averaging formulas, the pull-back used in the variation of constants formula must be computed. From Agrachev and Gamkrelidze [1], we have

$$(\Phi_{0,t}^g)^* f = f + \textstyle\sum_{k=0}^{\infty} \int_0^T \cdots \int_0^{s_{k-1}} \left(\mathrm{ad}_{g(s_k)} \cdots \mathrm{ad}_{g(s_1)} f\right) ds_k \ldots ds_1$$

where the $\{s_j\}$ represent time. The convergence of the infinite sum can be problematic, however if we introduce the following assumption

$$[Y_c, [Y_b, [Y_a, S]]] = 0 \tag{6}$$

it becomes of finite order. Although this may seem to be limiting, the homogeneous structure of Lagrangian mechanical systems satisfies the above assumption in all cases. There is also a larger classes of systems for which the above assumption holds.

Assume the input functions $v^a(t)$ in Eq. (2) are $T$-periodic with the properties $\int_0^T v^a(s_1)ds_1 = 0$ and $\int_0^T \int_0^{s_2} v^a(s_1)ds_1 ds_2 = 0$. Namely, the input function is cyclic with zero mean. For convenience, define the autonomous matrix $V = \mathrm{V}^{ab}$ by

$$\mathrm{V}^{ab} = \tfrac{1}{2T}\int_0^T \left(\int_0^{s_1} v^a(s_1)ds_2\right)\left(\int_0^{s_2} v^b(s_1)ds_2\right)ds_1$$

and the time average of a matrix function by

$$\overline{V}(t) = \tfrac{1}{T}\int_0^T V(t)dt.$$

We will also have the following notation

$$\mathrm{V}^{(a)}_{(n)}(t) = \int_0^t \int_0^{s_{n-1}} \cdots \int_0^{s_2} v^a(s_1)ds_1 \cdots ds_{n-1}.$$

For the case where there are multiple upper and lower indices, the tensor is the product of the above type of integral. An example is $\mathrm{V}^{(a,b)}_{(1,1)}(t)$:

$$\mathrm{V}^{(a,b)}_{(1,1)}(t) = \mathrm{V}^{(a)}_{(1)}\,\mathrm{V}^{(b)}_{(1)} = \left(\int_0^t v^a(s_1)ds_1\right)\left(\int_0^t v^b(s_1)ds_1\right)$$

Note that $V^{ab} = \frac{1}{2}\overline{\mathrm{V}^{(a,b)}_{(1,1)}(t)}$. Additionally, define $\tilde{\mathrm{V}}^{(a)}_{(n)} = \mathrm{V}^{(a)}_{(n)} - \overline{\mathrm{V}^{(a)}_{(n)}}$, and for the multi-index version $\tilde{\mathrm{V}}^{(A)}_{(N)} = \mathrm{V}^{(A)}_{(N)} - \overline{\mathrm{V}^{(A)}_{(N)}}$ where $(A) = (a_1, a_2, ..., a_{|A|})$ and $(N) = (n_1, n_2, ..., n_{|N|})$.

**Theorem 1 (Second order averaging [21])** *Consider system (2) and the initial value problem*

$$\begin{aligned}\dot{z} &= S(z) + \overline{Y_0(z)} - D(z) - \mathrm{V}^{ab}\,\langle Y_a : Y_b\rangle \\ &+\tfrac{1}{2}\epsilon\,\overline{\mathrm{V}^{(a,b)}_{(2,1)}(t)}\,[[Y_a, S+Y_0-D],[Y_b, S+Y_0-D]] \\ &-\tfrac{1}{2}\epsilon\left(\overline{\mathrm{V}^{(a,b,c)}_{(2,1,1)}(t)} - \overline{\mathrm{V}^{(a)}_{(2)}}\;\overline{\mathrm{V}^{(b,c)}_{(1,1)}}\right)\cdot\langle Y_a : \langle Y_b : Y_c\rangle\rangle \\ &+\tfrac{1}{4}\epsilon\left(\overline{\tfrac{1}{2}\int_0^t \mathrm{V}^{(a,b)}_{(1,1)}(\tau)\mathrm{d}\tau\;\mathrm{V}^{(c,d)}_{(1,1)}(t)} - \overline{\int_0^t \tilde{\mathrm{V}}^{(a,b)}_{(1,1)}(\tau)\mathrm{d}\tau}\;\overline{\mathrm{V}^{(c,d)}_{(1,1)}(t)}\right)\cdot[\langle Y_a : Y_b\rangle, \langle Y_c : Y_d\rangle]\end{aligned} \tag{7}$$

*with $z(0) = z_0$. If the control vector fields and input forcing are smooth functions of their respective arguments and that the iterated Lie bracket properties of (2) and (6) hold, then $q(t) - \Phi^g_t(z(t)) = O(\epsilon)$ as $\epsilon \to 0$ on the time scale 1, and $q(t) - \Phi^g_t(z(t)) = O(\epsilon)$ as $\epsilon \to 0$ for all $t$, if $z = 0$ is an asymptotically stable critical point for the linear approximation of the system in (7).*

Note that in the situation where system behavior can be captured with only first order effects, the second order symmetric products in the theorem disappear. In that case the result simplifies to the expected first order averaging as discussed in [4].

### 3.2 Trajectory Stabilization

Given a configuration controllable system (see [9] for a discussion of configuration controllability) of the form (2), we would like to choose appropriate oscillatory feedback controls to either stabilize the system or track a trajectory. To this end, we will apply Thm. 1 using controls with amplitudes generated by a discretized system error signal and show that a linearization of the result is stable under appropriate choice of gain constants.

If the system (2) is configuration controllable, we know that there exists a set of linearly independent vector fields $Y_a$, $\langle Y_a : Y_b\rangle$, $\langle Y_a : \langle Y_b : Y_c\rangle\rangle$ that span $\mathbb{R}^n$ (for details see [9, 5]). As shown in [21], for the elements $Y_{ab} = \langle Y_a : Y_b\rangle$ from this set define

$$\zeta^a_{ab} = \alpha_{ab}\sin(\lambda_{ab}t),\ \zeta^b_{ab} = -\sin(\lambda_{ab}t) \tag{8}$$

and for the elements $Y_{abc} = \langle Y_a : \langle Y_b : Y_c\rangle\rangle$ define

$$\xi^a_{abc} = \xi^b_{abc} = -\cos(\mu_{abc}t),\ \xi^c_{abc} = \beta_{abc}\cos(2\mu_{abc}t) \tag{9}$$

where $\lambda_{ab}, \mu_{abc} \in \mathbb{Z}^+$ and the $\alpha_{ab}, \beta_{abc}$ are scalar constants. Define a lexigraphical ordering on the pairs $ab$ and triples $abc$ such that $ab < cd$ if $a \le c$ and $b < d$ and similarly for $abc$. Then choose the frequencies $\lambda_i = \lambda_{i-1} + 1$, $\mu_1 = \lambda_{m-1,m} + 1$, and $\mu_i = 2\mu_{i-1} + 1$. Now sum the appropriate components for each vector field to get the control functions

$$u^a(t) = \textstyle\sum_{ij}\zeta^a_{ij} + \sum_{ijk}\xi^a_{ijk}$$

which have the form

$$\begin{aligned}u^a(t) = &\textstyle\sum_i \alpha_i\cos(\lambda_i t) - \sum_j \cos(\lambda_j t) \\ &+\textstyle\sum_k \beta_k\cos(2\mu_k t) - \sum_l \cos(\mu_l t).\end{aligned}$$

By direct computation one can check that $\overline{V^{(a,b)}_{(2,1)}} \equiv 0$. Also, note that for simple mechanical systems the last term in the summation of (7) is identically zero. The averaged system will then have the form

$$\begin{aligned}\dot{z} &= S(z) + Y_0(z) - D(z) - \mathrm{V}^{ab}\,(\alpha,\beta)\,\langle Y_a : Y_b\rangle \\ &-\frac{1}{2}\epsilon\left(\overline{\mathrm{V}^{(a,b,c)}_{(2,1,1)}} - \overline{\mathrm{V}^{(a)}_{(2)}}\;\overline{\mathrm{V}^{(b,c)}_{(1,1)}}\right)(\alpha,\beta)\cdot\langle Y_a : \langle Y_b : Y_c\rangle\rangle\end{aligned}$$

which we can rewrite as

$$\dot{z} = S(z) + Y_0(z) - D(z) + B(z)H(\alpha,\beta)$$

where

$$B(z) = \left[\langle Y^a : Y^b\rangle, \langle Y_a : \langle Y_b : Y_c\rangle\rangle\right]$$

$$H(\alpha,\beta) = \begin{bmatrix} -\overline{V^{ab}_{11}} \\ -\frac{1}{2}\epsilon\left(\overline{V^{abc}_{211}} - \overline{V^{(a)}_{(2)}}\;\overline{V^{(b,c)}_{(1,1)}}\right)\end{bmatrix}.$$

**Theorem 2 ([21])** *Consider a mechanical system of the form (2), which is configuration controllable with first*

*and second level symmetric products, and where the dimensions of the spaces spanned by* $Y_a$, $\langle Y_a : Y_b \rangle$, *and* $\langle Y_a : \langle Y_b : Y_c \rangle\rangle$ *are respectively,* $m$, $n_{ab}$, *and* $n_{abc}$. *Assume that there exist functions of the form (8) and (9) such that the linearization of* $H(\alpha, \beta)$ *with respect to* $\alpha$ *and* $\beta$ *is invertible on the subspace to control, and let* $z(t)$ *be the averaged system response. Then there exists* $K \in \mathbb{R}^{(n_{ab}+n_{abc})\times 2n}$ *such that for*

$$\begin{bmatrix} \alpha \\ \beta \end{bmatrix} = -Kz(T\lfloor t/T \rfloor)$$

*where* $\alpha \in \mathbb{R}^{n_{ab}}$, $\beta \in \mathbb{R}^{n_{abc}}$, *we have the stabilized average system response* $\lim_{t\to\infty} z(t) = 0$.

Note that this theorem stabilizes an equilibrium point of our averaged system while the original system will, in general, tend to oscillate about this equilibrium point. Given that as a fish swims, the flapping of the tail causes a reactive oscillation in the body, this relation seems reasonable for our purposes.

## 4 System Analysis and Results

The theory described above has been implemented both in simulation and in experiment. We first describe our experimental apparatus, and then summarize our simulation and experimental studies.

### 4.1 Experimental Apparatus

Our robotic "fish" prototype consists of three rigid links suspended from a low friction carriage. Fig. 2 shows a top view schematic and photograph, while Fig. 3 shows the analogous side views. The system consist of a main body link, a rectangular tail link, and a narrow supporting arm between the body and tail that is analogous to the peduncle of real fish. The carriage's supporting structure rests upon two orthogonal sets of rails and a rotating platform, all supported on low friction bearings. The peduncle and tail links are driven independently by two D.C. servo motors mounted on the moving carriage. With this carriage mechanism, undulations of the tail and peduncle enable the fish to propel itself with three degrees of planar movement around its 4' wide by 4' deep by 36' long water tank. The carriage's frictional drag is sufficiently low so that this system is a reasonable approximation to untethered swimming. A more detailed description of this system can be found in [14], where we show that this system operates in fluid regimes which are typical of biological fish.

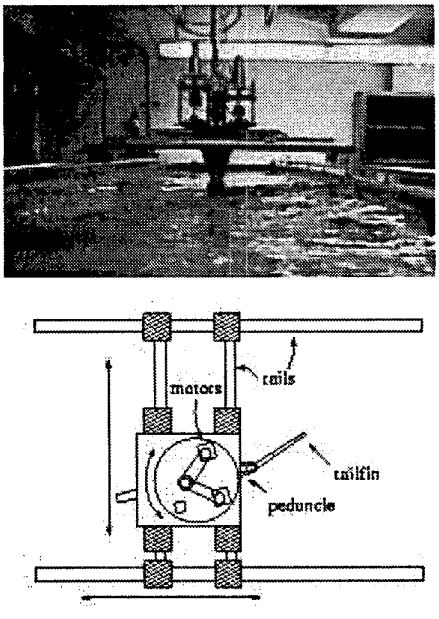


**Figure 2:** Rear photograph and top view schematic.

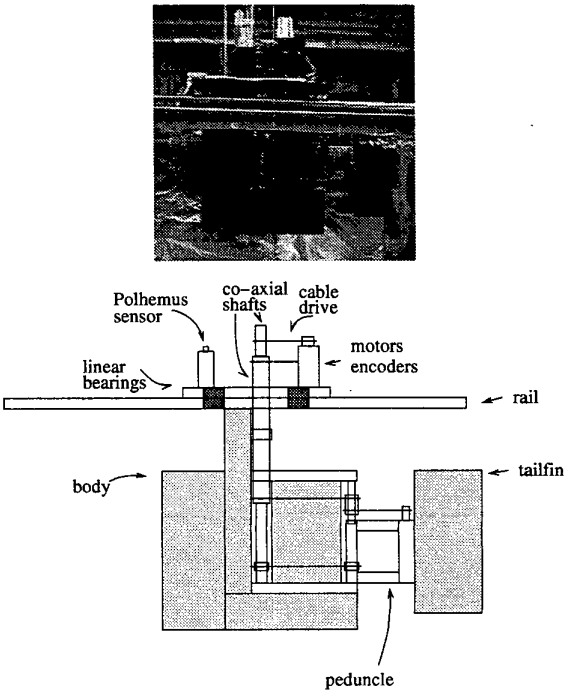


**Figure 3:** Side view photograph and schematic.

### 4.2 Results

In a previous paper [15], we presented motion planning results for our fish robot using open loop controls of the form (8)-(9). In Figs. 4-5 we show simulated and experimental open loop response to the use of a forward swimming gait. As can be seen, in the experimental data, when running without feedback, the robot will not swim down the center of the tank, but runs into one of the tank walls and moves along it. The body oscillation and lateral motion agree well between simulation and experiment, however the robot physically only moves about half the distance shown in the simulation. This difference is most likely accounted for with unmodeled terms such as skin friction which would act to slow the simulated system in the forward direction.

The accuracy of trajectory tracking with open-loop con-

trols is highly sensitive to initial conditions. As one would expect when applying such methods to physical systems, exact initial conditions cannot be easily set, and disturbances to the physical system cause it to wander from the intended trajectory. To apply the second-order results of Thm. 2, we must know what motions of the fish correspond to which symmetric products. From [15] we know that the forward motion corresponds to a first-level product. The turn and lateral motion are coupled as a second-level product. The full result of Thm. 2 requires that we use both of these gaits simultaneously to correct for errors in position. Unfortunately the actuators on our experimental apparatus do not have sufficient bandwidth to generate both first and second order maneuvers simultaneously. However, with a slight modification of the theory, we can use the first order version of Thm. 2 to achieve a preliminary verification of the tracking result.

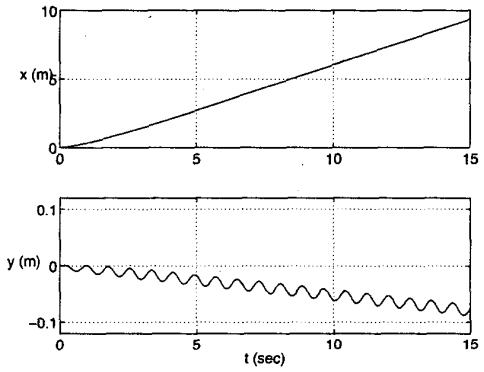


**Figure 4:** Simulated open-loop robot behavior.

To eliminate the errors induced by mismatched initial conditions and system disturbances, we applied the restricted first-order results of Thm. 2 to stabilize the fish robot's motions about a trajectory down the center of the tank. The controls for corrective maneuvers are given by:

$$\begin{aligned}\psi_1(t) &= 0.4\,(err + \sin(8(t - \arcsin(err)))\\ \psi_2(t) &= 0.4\cos(8t)\,,\end{aligned}$$

where $err = k_p y + k_d \dot{y}$ is sampled every time-period, thus remaining constant over the period of a tail stroke and satisfying the requirements of Thm. 1. Intuitively, these controls modify the forward motion of the fish by superimposing a turn via a shift in the median of the tail oscillation. In this way the turn enters in through a first level symmetric product. The effect of the error term is to bias the peduncle tail toward one side of the fish. The direction and magnitude of the bias depends on the sign of the error term. This first order control strategy is addressed using the second order theorem by ignoring the higher order terms. We further simplified this controller for use in experiment to have the form

$$\psi_1(t) = 0.4\sin(8t) + (err)\,,\ \psi_2(t) = 0.4\cos(8t) + (err)$$

(note that both joint angles are measured relative to the body orientation) and the error was updated to correspond to the previous period backwards from each time step rather than being updated only at the end of each period. The end result of these differences is roughly the same as in the simulation: the average value of the peduncle angle is shifted to produce changes in lateral motion.

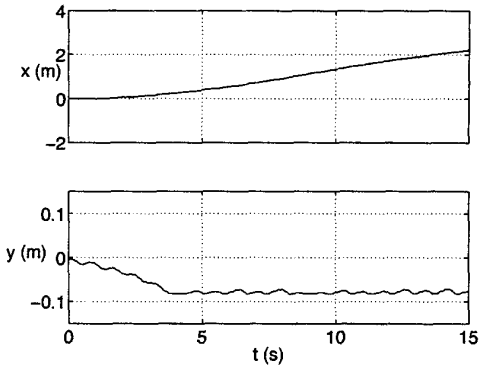


**Figure 5:** Experimental open-loop robot behavior.

Simulation results of this feedback strategy can be seen in Fig. 6 and experimental results in Fig. 7. The gains for the experiment are $k_p = 15.3$ and $k_d = 3.1$. For the simulation we used $k_p = 5$ and $k_d = 8$. The difference in gains was chosen partly to compensate for the difference in control strategy and partly to compensate for the differences in the open-loop results so that the closed loop qualitative results would better agree. Recall that these differences are most likely due to neglected dissipative terms in the model. The lighter damping of the simulation does not require the larger experimental gain magnitudes in order to achieve similar stabilization results. The dashed line in the experimental lateral motion plot represents the averaged feedback signal. The simulation initial conditions, $(x, y, \theta) = (0, -0.1, 0)$, are similar to the experiment position at $t = 1s$. The discrepancies between the simulation and experiment can be partially explained by unmodeled drag terms (only form drag is included in this model) which, from the open loop trajectory results can be seen to have a significant effect, and are partially due to mismatches in the initial conditions. Given the lack of an integral control term, both the simulation and experiment demonstrate a nonzero steady-state lateral position. In the simulation, with the lower gain values, this steady state value is larger than in the experiment. At steady state in the experiment, the average deviation from the centerline is less than or equal to approximately 0.5 cm. In spite of the discrepancies, the trajectories do seem to support each other. Moreover, the experimental results clearly demonstrate stabilization of fish's movement to a straight line trajectory.

## 5 Conclusions and Future Work

This paper reviewed a general approach for designing oscillatory controls for mechanical systems, and its partic-

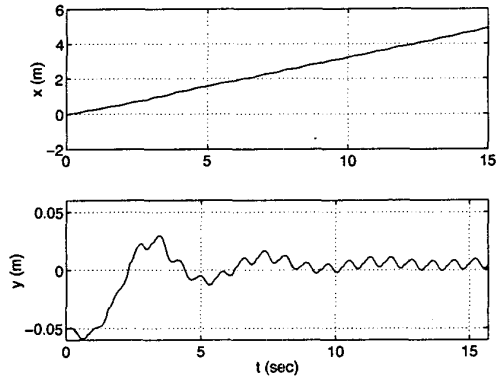


**Figure 6:** Simulated robot behavior with lateral feedback.

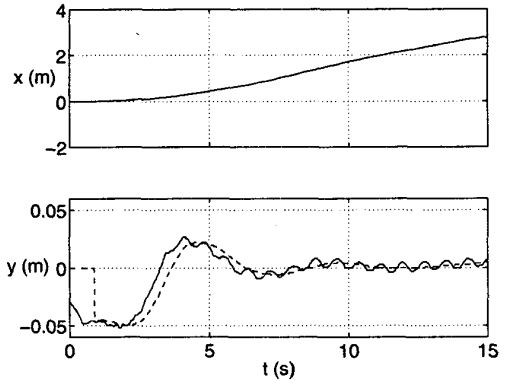


**Figure 7:** Experimental robot behavior with lateral feedback.

ular application to the feedback control of a highly nonlinear, underactuated carangiform-type robot. The use of this type of feedback was shown to work quite well in simulation, and a slightly modified version of the controller demonstrated convergence to a simple forward swimming trajectory in experiment. Our ongoing work focuses on better fluid models (to which our general control design approach still applies), while also addressing issues of actuator bandwidth in oscillatory control, and achieving simultaneous tracking in multiple dimensions.

## References

[1] A. Agrachev and R. Gamkrelidze. The exponential representation of flows and the chronological calculus. *USSR Sbornik*, 35(6):727–85, 1978.

[2] J.M. Anderson and P.A. Kerrebrack. The vorticity control unmanned undersea vehicle–an autonomous vehicle employing fish swimming propulsion and maneuvering. In *Proc. 10th Int. Sym. Unmanned Untethered Submersible Tech.*, pages 189–95, Durham, NH, Sep. 1997.

[3] D. Barrett, M. Grosenbaugh, and M.S. Triantafyllou. The optimal control of a flexible hull robotic undersea vehicle propelled by an oscillating foil. In *Proc. 1996 Symp. Aut. Underwater Veh. Tech.*, pages 1–9, 1996.

[4] F. Bullo. Averaging and vibrational control of mechanical systems. *SIAM J. Contr. Optim.*, 2001. submitted for publication.

[5] F. Bullo, N.E. Leonard, and A.D. Lewis. Controllability and motion algorithms for underactuated Lagrangian systems on Lie groups. *IEEE Trans. Aut. Contr.*, 45(8):1437–54, 2000.

[6] I.-M. Chen, H.-S. Li, and A. Cathala. Amoebot – metamorphic underwater vehicle. In *Fifth International Conference on Control, Automation, Robotics, and Vision*, Singapore, 1998.

[7] S. Childress. *Mechanics of Swimming and Flying.* Cambridge University Press, Cambridge, 1981.

[8] S.D. Kelly, R.J. Mason, C.T. Anhalt, R.M. Murray, and J.W. Burdick. Modelling and experimental investigation of carangiform locomotion for control. In *Proc. Amer. Contr. Conf.*, pages 1271–6, 1998.

[9] A.D. Lewis and R.M. Murray. Configuration controllability of simple mechanical control systems. *SIAM J. Contr. Optim.*, 35(3):766–90, 1997.

[10] P.Y. Li and S. Saimek. Modeling and estimation of hydrodynamic potentials. In *Proc. 38th IEEE Conf. Dec. Cont.*, pages 3253–8, 1999.

[11] J.L. Lighthill. *Mathematical Biofluiddynamics.* SIAM, Philadelphia, 1975.

[12] R.J. Mason and J.W. Burdick. Construction and modelling of a carangiform robotic fish. In *Proc. 1999 Int. Symp. Exp. Rob.*, pages 235–42, 1999.

[13] R.J. Mason and J.W. Burdick. Propulsion and control of deformable bodies in an ideal fluid. In *Proc. IEEE Int. Conf. Rob. Aut.*, pages 773–80, 1999.

[14] R.J. Mason and J.W. Burdick. Experiments in carangiform robotic fish locomotion. In *Proc. IEEE Int. Conf. Rob. Aut.*, pages 428–35, 2000.

[15] K.A. Morgansen, V. Duindam, R.J. Mason, J.W. Burdick, and R.M. Murray. Nonlinear control methods for planar carangiform robot fish locomotion. In *Proc. IEEE Int. Conf. Rob. Aut.*, 2001.

[16] P. Morin, J.-B. Pomet, and C. Samson. Design of homogeneous time-varying stabilizing control laws for driftless controllable systems via oscillatory approximation of Lie brackets in closed loop. *SIAM J. Contr. Optim.*, 38(1):22–49, Dec. 1999.

[17] J.N. Newman and T.Y. Wu. Hydrodynamical aspects of fish swimming. In T. Wu, C. Brokaw, and C. Brennen, editors, *Swimming and Flying in Nature, Vol 2.*, pages 615–34. Plenum Press, New York, 1975.

[18] S. Saimek and P.Y. Li. Motion planning and control of a swimming machine. In *Proc. Amer. Contr. Conf.*, pages 125–30, 2001.

[19] A.R. Teel, R.M. Murray, and G. Walsh. Nonholonomic control systems: From steering to stabilization with sinusoids. In *Proc. 31st IEEE Conf. Dec. Contr.*, pages 1603–9, 1992.

[20] M.S. Triantafyllou and G.S. Triantafyllou. An efficient swimming machine. *Scientific American*, pages 64–70, Mar. 1995.

[21] P.A. Vela, K.A. Morgansen, and J.W. Burdick. Second order averaging methods for oscillatory control of underactuated mechanical systmes. to appear in Proceedings of the 2002 American Control Conference, 2002.

[22] M.J. Wolfgang, J.M. Anderson, M.A. Grosenbaugh, D.K.P. Yue, and M.S. Triantafyllou. Near-body flow dynamics in swimming fish. *J. Exp. Biology*, 202(17):2303–7, 1999.